

QUANTUM DOTS SOLAR CELLS BASED ON CdS/CdSe/ZnS-TiO₂ PHOTOANODES

ABSTRACT

Quantum dots solar cells (QDSSCs) based on the different CdS/CdSe/ZnS-TiO₂ photo anodes were prepared by successive ionic layer adsorption and reaction (SILAR) processes. The CdS, CdSe and ZnS layers were considered by UV-Vis spectrum for optical and the SILAR cycles of CdS, CdSe and ZnS show different impact on the performance of QDSSCs. With the deposition times of CdS increasing (from 1 to 5 cycles), the short circuit current density of the device is enhanced. On the contrary, the increasing deposition times of CdSe (from 1 to 5 cycles) has a negative effect for the generation and collection of photoelectron. In addition, the electrochemical impedance spectroscopy technology (EIS) was used to investigate the diffusion and recombination in QDSSCs. In addition, the dynamic resistances was discussed based on the EIS results.

Keywords: Quantum dots, solar cells, photo anodes.

I. INTRODUCTION

Quantum dot-sensitized solar cells (QDSSCs) are considered as a promising low-cost alternative for third generation photovoltaic [1]. This solar cell is sourcing from the dye-sensitized solar cell (DSSC), which is based on sandwich dye-sensitized nano crystalline work electrode, counter-electrode and electrolyte. Compared to the conversional DSSC, the sensitizer of QDSSC is replaced by semiconductor quantum dots (QDs) such as CdS [2], PbS [3], Ag₂S [4], CdSe [5], Ag₂Se [6], CdTe [7] and InAs [8] which possess multiple advantages as tunable band gaps, high extinction coefficient, and high photo stability [9-11]. Unfortunately, QDSSC which promises a high theoretical efficiency up to 44% for its special multi electrons generation character [12], still presents lower energy conversion efficiency and far below the theoretical value. For QD-sensitizers, CdS, CdSe and ZnS have been paid much attention because of their high potential in photo absorption under visible region. The two materials exhibit different characteristics. For CdS, its conduction band (CB) edge is higher than that of TiO₂, making the electron injection from CdS to TiO₂ very effective, but the absorption range of CdS is too narrow, which restrict the utilization of light. Lee and Lo [13], model system prepared by SILAR is favorable than single CdS or CdSe, which can extend spectral response to the visible light region and charge injection from QDs to TiO₂. The influence of SILAR cycles on the performance has also been investigated recently [14]. However, the detailed optical and especially electrochemical properties of the photo anodes with different SILAR cycles are still lack of deep research. In this paper, we prepared CdS/CdSe/ZnS co-sensitizer on meso porous TiO₂ surfaces with different SILAR cycles. The optical properties of the photo anodes and the photovoltaic performance of the corresponding solar cells were investigated. Moreover, EIS was employed to investigate the interface impedance and chemical capacitance of QDSSCs. Based on the EIS results, the SILAR deposition cycles effect on the charge recombination was discussed.

II. EXPERIMENT

Materials. Cd(CH₃COO)₂·2H₂O (99%), KCl, Na₂S, Zn(NO₃)₂, Se powder, S powder, Na₂SO₃, TiCl₄, TiO₂ paste obtained from Dyesol, Australia.

To prepare TiO₂ films, the TiO₂ thin films were fabricated by silk-screen printing with commercial TiO₂ paste. Their sizes ranged from 10 to 20 nm. Two layers of film with thickness of 8 μm (measured by microscope). Then, the TiO₂ film was heated at 400°C for 5 min, 500°C for 30 min. Afterward, the film was dipped in 40-mmol TiCl₄ solution for 30 min at 70°C and heated at 500°C for 30 min. The specific surface area of the mesoporous TiO₂ were investigated by using the N₂ adsorption and desorption isotherms before and after the calcination. The surface area is 120.6 m²g⁻¹ (measured by BET devices). This result indicates that the synthesized material has wider mesoporous structure.

48 **To prepare TiO₂/CdS/CdSe/ZnS films**, the highly ordered TiO₂ were sequentially sensitized with
 49 CdS, CdSe and ZnS QDs by SILAR method. First, the TiO₂ film was dipped in 0.5 mol/L
 50 Cd(CH₃COO)₂-ethanol solution for 5 min, rinsed with ethanol, dipped for 5 min in 0.5 mol/L
 51 Na₂S-methanol solution and then rinsed with methanol. The two-step dipping procedure corresponded
 52 to one SILAR cycle and the incorporated amount of CdS QDs was increased by repeating the assembly
 53 cycles for a total of three cycles. For the subsequent SILAR process of CdSe QDs, aqueous Se solution
 54 was prepared by mixing Se powder and Na₂SO₃ in 50ml pure water, after adding 1 mol/L NaOH at 70°C
 55 for 7h. The TiO₂/CdS samples were dipped into 0.5 mol/L Cd(CH₃COO)₂-ethanol solution for 5 min at
 56 room temperature, rinsed with ethanol, dipped in aqueous Se solution for 5 min at 50°C, rinsed with pure
 57 water. The two-step dipping procedure corresponds to one SILAR cycle. Repeating the SILAR cycle
 58 increases the amount of CdSe QDs (a total of four cycles). The SILAR method was also used to deposit
 59 the ZnS passivation layer. The TiO₂/CdS/CdSe samples were coated with ZnS by alternately dipping the
 60 samples in 0.1 mol/L Zn(NO₃)₂ and 0.1 mol/L Na₂S-solutions for 5 min/dip, rinsing with pure water
 61 between dips (a total of two cycles). Finally, it was heated in a vacuum environment with different
 62 temperatures to avoid oxidation (see Fig. 1). The TiO₂/CdS/CdSe/ZnS was measured thickness by
 63 microscopic. The results of the average thickness of CdS(1), CdSe(1), ZnS(1) are 40nm, 43.3nm, 40nm
 64 respectively.

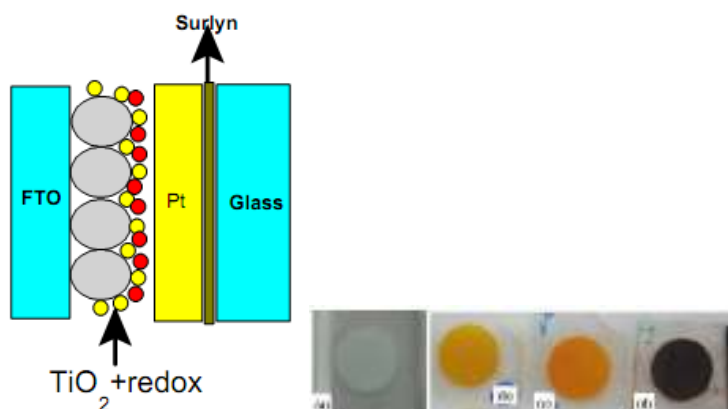


Figure 1. The diagram shows the instruction of the QDSSCs and images of photo anodes

Fabrication of QDSSCs:

The polysulfide electrolyte used in this work was prepared freshly by dissolving 0.5 M Na₂S, 0.2 M S, and 0.2 M KCl in Milli-Q ultrapure water/methanol (7:3 by volume). The CdS/CdSe/ZnS co-sensitized TiO₂ photoanode and Pt counter electrode were assembled into a sandwich cell by heating with a Surlyn. The electrolyte was filled from a hole made on the counter electrode, which was later sealed by thermal adhesive film and a cover glass. The active area of QDSSC was 0.38 cm².

Characterizations and measurements

The morphology of the prepared samples was observed using fieldemission scanning electron microscopy FE-SEM, S4800). The crystal structure was analyzed by an X-ray diffractometer (XRD) with CuKα radiation. The absorption properties of the samples were investigated by UV-vis spectrum (JASCO V-670). Photocurrent – Voltage measurements were performed on a Keithley 2400 sourcemeter using a simulated AM 1.5 sunlight with an output power of 100 mW/cm² produced by a solar simulator (Solarena, Sweden).

II. RESULTS AND DISCUSSION

65 Detailed morphological features and crystal of the pure TiO₂ and TiO₂/CdS/CdSe/ZnS photo anodes
 66 were investigated using TEM image. A typical TEM image of pure TiO₂ film is depicted in Fig. 2a.
 67 It is quite evident that the mean diameter of TiO₂ nanoparticle is about 25 nm. Fig. 2b shows a TEM
 68 image of the TiO₂/CdS/CdSe/ZnS photo anode prepared with the SILAR cycle number of CdS,
 69 CdSe and ZnS at 3, 3 and 2. We can clearly see that QDs uniformly cover the surface of TiO₂
 70 nanoparticles. It shows that the average diameter of QDs is from 2 nm to 3 nm. The results of the
 71

TEM demonstrate that the SILAR method is an efficient TiO_2 sensitization strategy for obtaining well covering the QDs on the TiO_2 surfaces.

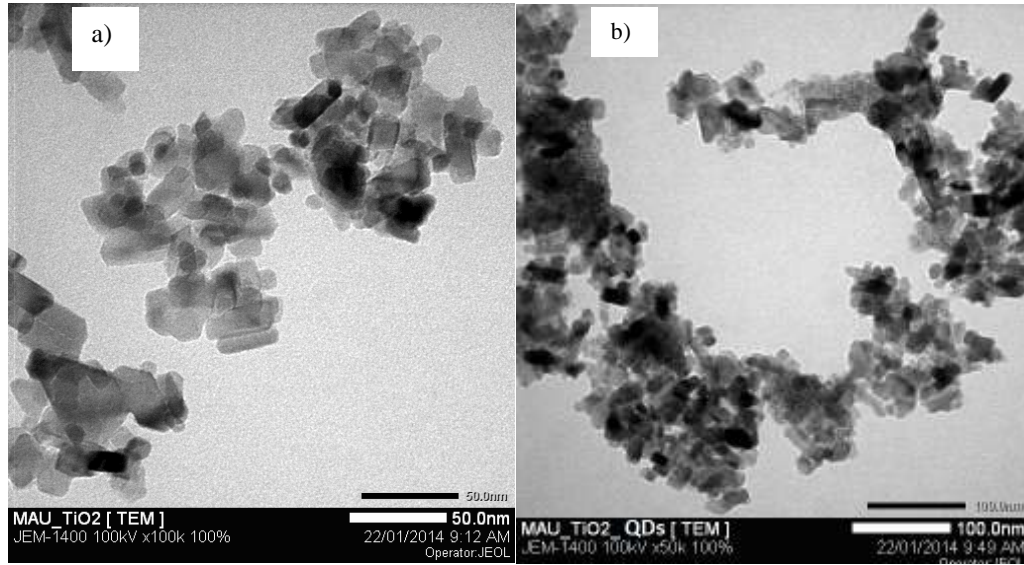


Figure 2. TEM images of (a) TiO_2 film and (b) $\text{TiO}_2/\text{CdS}/\text{CdSe}/\text{ZnS}$ film.

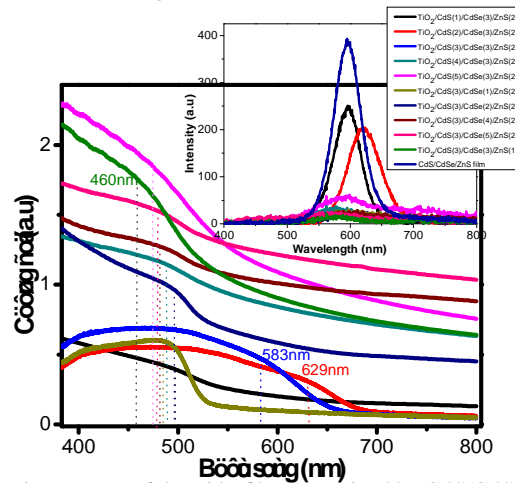


Figure 3. UV-Vis absorption spectra of the TiO_2 films sensitized by $\text{CdS}/\text{CdSe}/\text{ZnS}$ QDs shows the light absorption behavior of photoanodes changed with the SILAR cycles of CdS , CdSe and ZnS and Photoluminescence (PL) spectra of the $\text{TiO}_2/\text{CdS}/\text{CdSe}/\text{ZnS}$ (small image).

The optical performance of co-sensitized TiO_2 thin films can be monitored by studying the absorbance and energy band gap of the materials. Fig. 3a shows the UV-Vis spectrum of thus sensitized electrodes measured after each cycle of SILAR. As expected, the absorbance increased with the deposition cycles of CdS , CdSe and ZnS . However, only absorption spectra with SILAR cycles of the electrode $\text{TiO}_2/\text{CdS}(3)/\text{CdSe}(3)/\text{ZnS}(2)$ obtains the best efficiency as discussed in the following section. The change of absorbance is due to QDs that was loaded on TiO_2 film. Moreover, the increasing successive deposition cycles also caused a red shift of UV-Vis that losses by quantum confinement effect [15]. The average sizes of CdS , CdSe and ZnS are consistent with the FE-SEM images. The effect of deposition cycles of CdS , CdSe and ZnS can be clearly seen on the energy band gap values of $\text{CdS}/\text{CdSe}/\text{ZnS}$ co-sensitized TiO_2 films. The estimated band gaps vary from 1.97 eV to 2.7 eV, which are higher than the values reported for CdS and CdSe in bulk (2.25 eV and 1.7 eV [1], respectively), indicating that the sizes of CdS , CdSe and ZnS on TiO_2 films are still within the scale of QDs. A higher absorption is thus obtained because the absorption spectrum of ZnS complements those of the CdSe and CdS QDs. Furthermore, ZnS acts as a passivation layer to protect the CdS and CdSe QDs from photo corrosion [16]. Fig 3b shows the PL of different photoanodes that their thick is changed by the cycles SILAR.

After the CdS, CdSe, and ZnS QDs are sequentially deposited onto the TiO₂ film, a cascade type of energy band structure is constructed for the co-sensitized photo anode. The best electron transport path is from the CB of ZnS and CdSe to that of CdS, and finally, to TiO₂ film (shows Fig 6b). Thus, the PL of TiO₂/CdS/CdSe/ZnS was quenched (displayed in Figure 3b). This reveal that TiO₂ film serve as effective quenchers of excited CdS, CdSe and ZnS QDs. The thick photo anode film quenches more efficiently than thin photo anode film.

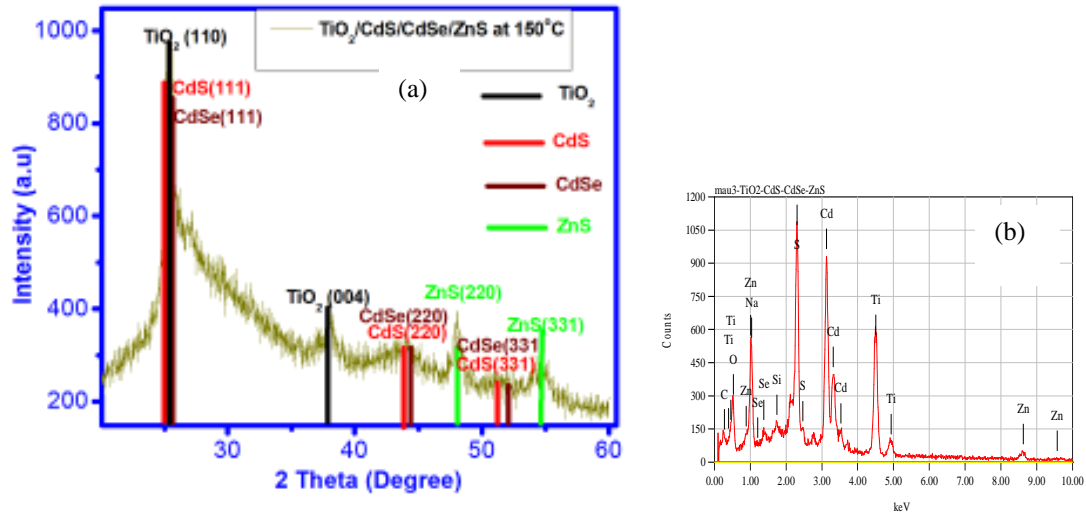


Figure 4. (a) XRD and (b) Energy dispersive X - ray spectrum (EDS) of TiO₂/CdS/CdSe/ZnS photo anodes.

The structure of the TiO₂/QDs photo electrodes for photovoltaic applications, shown in Fig. 4(a), are studied by the XRD patterns. It reveals that the TiO₂ have a anatase structure with a strong (101) peak located at 25.4°, which indicates that the TiO₂ film are well crystallized and grow along the [101] direction. Three peaks can be observed at 26.4°, 44° and 51.6°, which can be indexed to (111), (220) and (331) of cubic CdS, CdSe respectively. Two peaks can be observed at 48° and 54.6°, which can be indexed to (220) and (331) of cubic ZnS respectively. It demonstrates that the QDs have crystallized onto the TiO₂ film. Fig. 4(b) is the Raman spectrum of the TiO₂/QDs photo electrodes. It shows that an anatase structure of the TiO₂ films have five oscillation modes correspond to wave number at 143, 201, 395, 515 and 636 cm⁻¹. In addition, two peaks can be observed at 201, 395, and 515 cm⁻¹, which can be indexed to the cubic structure of CdS, CdSe. The results of the Raman is likely the results of XRD. Fig. 4 (b) is the energy dispersive X ray spectrum of the TiO₂/CdS/CdSe/ZnS film. It shows that the Ti and O peaks are from the TiO₂ film, Cd, Se, Zn and S peaks, clearly visible in the EDS spectrum, are from the QDs. The Si is from the FTO and C is from the solvent organic. That shows, the QDs are well deposited onto the TiO₂.

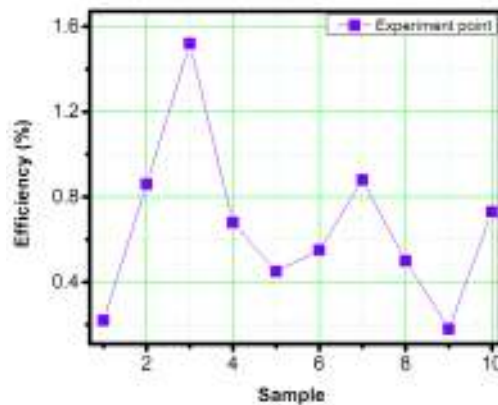


Figure 5.Diagram shows the values efficiency of solar cells.

In order to understand the effects of SILAR cycles of CdS, CdSe and ZnS, we prepared a series of combinations of CdS, CdSe and ZnS QDs on TiO₂ films, investigated their photovoltaic performances

with polysulfide electrolyte. All the samples were coated with ZnS to inhibit the recombination at the TiO₂ photo anode/polysulfide electrolyte interface [17]. Table 1 presents the photocurrent density voltage characteristics of the QDSSCs with different CdS/CdSe/ZnS co-sensitized TiO₂ films (active area of 0.38 cm²) at AM 1.5 (100 mW/cm²), and the related parameters of these QDSSCs are listed in Table 1. It shows that the power conversion efficiencies of QDSSCs are increasing with the SILAR cycle number of CdS, CdSe and ZnS at 3, 3 and 2, respectively. It is noted that lower power conversion efficiency was obtained for those cells with either less CdS and CdSe SILAR cycles than 3 or more CdS and CdSe SILAR cycles than 3 (shows Fig 5b). QDSSCs based on the TiO₂/CdS(3)/CdSe(3)/ZnS(2) photo anode shows an open-circuit voltage (V_{oc}) of 0.76 V, a short-circuit current density (J_{sc}) of 4.79 mA/cm², fill factor (FF) of 0.41 and an energy conversion efficiency (η) of 1.52%. As the deposition cycles of CdS and CdSe increase, there were slightly changes in V_{oc} and FF values. Besides, the J_{sc} decreases which cause in a reduced η (from 1.52% to 0.45%). These results indicate that better light absorption performance were obtained while more CdSe loaded on TiO₂/CdS. However, TiO₂/CdS/CdSe photo anode can increase recombination in QDSSCs. On the contrary, the increase of ZnS leads to the increasing generation of photoelectron and is helpful to collect excited electrons from ZnS, CdSe and CdS to TiO₂ film.

J_{sc} is given by equation:

$$J_{sc} = q \int b_s(E)QE(E)dE \quad (1)$$

J_{sc} is the photon current density and b_s(E) is the number of photons in the range E to E+dE per unit area per unit time. q is the charge of the electron, QE depends on the absorption coefficient of the material solar cell. The short-circuit current depends on a number of factors: the area of the solar cell, the number of photons, the spectrum of the incident light, the optical properties (absorption and reflection) and the collection probability of the solar cell, which depends chiefly on the surface passivation and the minority carrier lifetime in the base. From Equation 1, we see that the J_{sc} is not directly dependent on the thickness of the layer of QDs. When the thickness of the layer of QDs changes, the results change the absorption spectrum and the collection probability of the solar cell. After all, they cause change of J_{sc}, however, this change is nonlinear.

An equation for V_{oc} is found by setting the net current equal to zero in the solar cell equation to give:

$$V_{oc} = \frac{kT}{q} \ln \left(\frac{I_L}{I_0} + 1 \right) \quad (2)$$

The above equation shows that V_{oc} depends on the saturation current of the solar cell and the light-generated current. The saturation current, I₀ depends on recombination in the solar cell. Open-circuit voltage is then a measure of the amount of recombination in solar cells. FF depend on V_{oc} values, the junction quality (related with the series R_s) and the type of recombination in a solar cell. From Table 1, V_{oc} values change according to the film thickness from 0.29 to 0.76, corresponding to the change in FF from 0.26 to 0.41. Therefore the FF is the low value because V_{oc} is low. On the other hand, V_{oc} depend on the recombination process, particularly they are large, it gives low open-circuit voltages. In addition, FF is effected by R_s. The equations of R_s can be calculated by Thongprun and co-workers [18].

$$R_s = \frac{V_1 - V_2}{I_2 - I_1} - \frac{1}{\lambda(I_2 - I_1)} \ln \left[\frac{I_{ph} + I_o - I_1}{I_{ph} + I_o - I_2} \right] \quad (3)$$

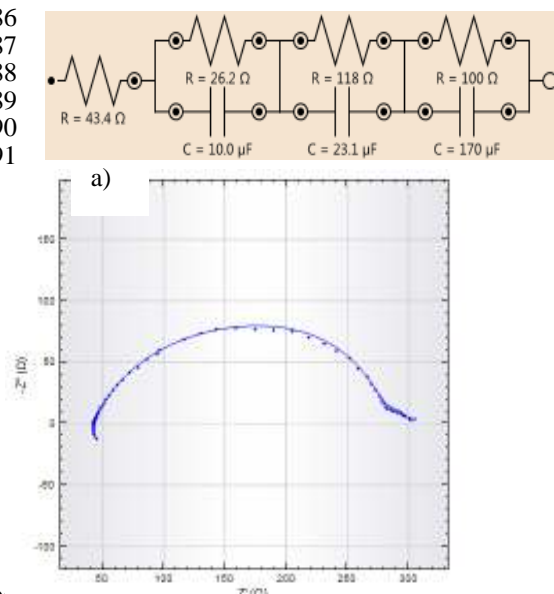
Two operating points (I₁, V₁) and (I₂, V₂) on a single I-V curve. $\lambda = \frac{q}{nKT}$; I_{ph}, I_o are the photocurrent and the diode reverse saturation current. R_s values are calculated from 55 to 158 mΩcm². This values is large as result as low FF.

Table 1. Photovoltaic performance parameters of QDSSCs based on different photo anodes.

Samples	J_{SC} (mA/cm ²)	V_{OC} (V)	Fill factor FF	Efficiency η (%)
1	2.18	0.29	0.35	0.22
2	4.28	0.54	0.37	0.86
3	4.79	0.76	0.41	1.52
4	5.73	0.39	0.31	0.68
5	3.05	0.45	0.32	0.45
6	6.05	0.356	0.26	0.55
7	4.21	0.55	0.38	0.88
8	3.30	0.48	0.31	0.50
9	2.08	0.33	0.27	0.18
10	7.03	0.39	0.26	0.73

QDSSCs based on TiO₂/CdS/CdSe/ZnS photo anode have obtained a better efficiency than both QDSSCs based on TiO₂/CdS and TiO₂/CdSe photo anodes [19]. The result shows that the excited electrons have injected from conduction band (CB) of CdSe QDs to CB of TiO₂ in which they may not be effective because of the quasi Fermi levels (E_F) of CdSe being lower than that of TiO₂ [13]. On the other hand, the E_F of CdS QDs is higher than that of the TiO₂ [20], so it has improved the electrons injection from CdSe to TiO₂. In addition, a ZnS layer was coating to form a potential barrier between the QDs and the electrolyte, which blocks the electrons in the CB from recombination with the electrolyte [21]. Resulting in a high performance of efficiency. Because the E_F of CdS is higher than of TiO₂, beneficial effects are conferred to the coupled QDSSC system. From Table 1, it is evident that the photocurrent density of the coupled QDSSC was influenced by CdS/CdSe/ZnS co-sensitization cycles [22], which can be explained in two ways. Firstly, particle size variation in CdS, CdSe and ZnS QDs leads to E_F alignment and consequently, so the CB of CdS, CdSe, ZnS is higher than that of TiO₂. As a result, the excited electrons were transferred to TiO₂ easier [23].

184
185
186
187
188
189
190
191



19
193
194
195
196
197
198
199
200
201
202
203
204
205
206
207
208
209

Figure 6. (a) Nyquist plots of QDSSCs based on $\text{TiO}_2/\text{CdS}(3)/\text{CdSe}(3)/\text{ZnS}(2)$ photo anode, (b) Bode plot and (c) the proposed energy band structure of QDSSCs[15].

In order to research the dynamic processes in the QDSSCs, we have measured EIS plot under dark conditions at varying negative applied bias (0.7–0 V). Figure 6a shows the Nyquist plots of the $\text{CdS}(3)/\text{CdSe}(3)/\text{ZnS}(2)$ QDs - sensitized solar cells. There are two semicircles at Nyquist at high frequency and low frequency. The small semicircle at high frequency corresponds to the resistance movement of excited electrons at counter electrode/electrolyte (R_{ct1}) interface and FTO/ TiO_2 interface. The large semicircle at low frequency from 10–100 kHz described resistance against the movement of excited electron in TiO_2 and recombination at $\text{TiO}_2/\text{QDs}/\text{electrolyte}$ (R_{ct2}) interface and against inside the diffusion in electrolyte (Z_w). From Figure 6a, we see that the 200 Ω of R_{ct2} defined large, so it causes resistance the movement of electrons at the $\text{TiO}_2/\text{QDs}/\text{electrolyte}$ interface and recombination of the electrons in polysulfide [22]. The figure 6b shows that the Bode plot with $\text{TiO}_2/\text{CdS}(3)/\text{CdSe}(3)/\text{ZnS}(2)$ photo anode that is illuminated with an 1000 W/m^2 . At low frequency peaks corresponds to the movement of electrons at $\text{TiO}_2/\text{QDs}/\text{electrolyte}$ interface, while the peak at higher frequencies describe the movement of electrons at the Pt/electrolyte interface. Lifetime of electrons in semiconductor (τ_e) is determined by the following formula $= 1/2\pi f_{\text{max}}$. The f_{max} is the peak of the Bode plot at low frequencies, $\tau_e \sim 3.2 \text{ ms}$.

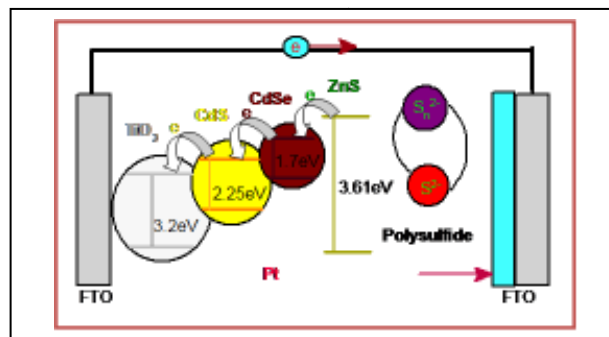
210 IV. CONCLUSIONS

211 We have successfully fabricate solar cells based on $\text{CdS}/\text{CdSe}/\text{ZnS}-\text{TiO}_2$ photo anodes which is
212 researched the optical to depend on number of CdS, CdSe and ZnS SILAR cycles. With the deposition
213 times of CdS increasing (from 1 to 5 cycles), the short circuit current density of the device is enhanced.
214 On the contrary, the increasing deposition times of CdSe (from 1 to 5 cycles) has a negative effect for the
215 generation and collection of photoelectron. For EIS spectrum, the SILAR deposition cycles effect on the
216 charge recombination of excited electrons in TiO_2 and TiO_2/QDs interfaces. The synthesized
217 $\text{TiO}_2/\text{CdS}/\text{CdSe}/\text{ZnS}$ photo anode exhibits a maximum efficiency value of 1.52%.

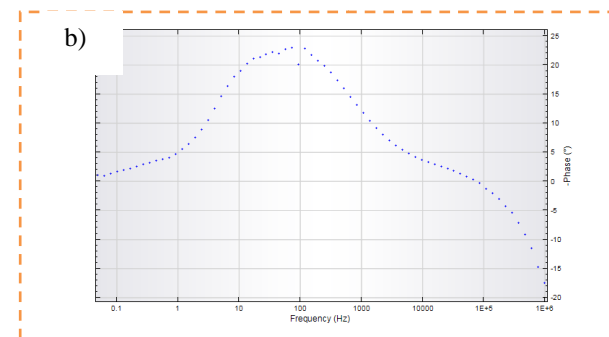
218 REFERENCES

- 219 [1]. Grätzel, Michael. "Photoelectrochemical cells." Nature 414.6861 (2001): 338-344
220 [2]. K. G. U. Wijayantha, L. M. Peter, L. C. Otley, Sol. Energy Mater. Sol. Cells **83** (2004) 363.
221 [3]. H. J. Lee, H. C. Leventis, S. J. Moon, P. Chen, S. Ito, S. A. Haque, T. Torres, F. Nüesch, T. Geiger, S. M.
222 Zakeeruddin, M. Grätzel, M. K. Nazeeruddin, Adv. Funct. Mater. **19** (2009) 2735.
223 [4]. A. Tubtimtae, K. L. Wu, H. Y. Tung, M. W. Lee, G. J. Wang, Electrochem. Commun. **12** (2010) 1158.
224 [5]. N. Fuke, L. B. Hoch, A. Y. Kaposov, V. W. Manner, D. J. Werder, A. Fukui, N. Koide, H. Katayama, M.
225 Sykora, ACS Nano **4** (2010) 6377.

c)



b)



226 [6]. A. Tubtimtae, M. W. Lee, G. J. Wang, J. Power Sources **196** (2011) 6603.
 227 [7]. J. H. Bang, P. V. Kamat, ACS Nano **3** (2009) 1467.
 228 [8]. P. R. Yu, K. Zhu, A. G. Norman, S. Ferrere, A. J. Frank, A. J. Nozik, J. Phys. Chem. B **110** (2006) 25451.
 229 [9]. S. Gorer, G. Hodes, J. Phys. Chem. **98** (1994) 5338.
 230 [10]. I. Moreels, K. Lambert, D. De. Muynck, F. Vanhaecke, D. Poelman, J. C. Martins, G. Allan, Z. Hens, Chem.
 231 Mater. **19** (2007) 6101.
 232 [11]. A. J. Nozik, J. Chem. Phys. Lett. **457** (2008) 3.
 233 [12]. M. C. Hanna, A. J. J. Nozik, J. Appl. Phys. **100** (2006) 074510.
 234 [13]. Y.L. Lee, Y.S. Lo, Adv. Funct. Mater. **19** (2009) 604
 235 [14]. V. Gonzalez-Pedro, X. Xu, I. Mora-Sero, J. Bisquert. Modeling high-efficiency quantum dot sensitized solar
 236 cells. ACS Nano 2010; **4**:5783–90.
 237 [15]. Pathan, H. M., and C. D. Lokhande. "Deposition of metal chalcogenide thin films by successive ionic layer
 238 adsorption and reaction (SILAR) method." Bulletin of Materials Science 27. **2** (2004): 85-111.
 239 [16]. Z. Tachan, M. Shalom, I. Hod, S. Ruhle, S. Tirosh, and A. Zaban, J. Phys. Chem. C **115**, 6162 (2011).
 240 [17]. Y. L. Lee, Y. S. Lo. Highly efficient quantum-dot-sensitized solar cell based on co-sensitization of CdS/CdSe.
 241 Advanced Functional Materials 2009; **9**:604–9.
 242 [18] J. Thongpron, K. Kirtikara, C. Jivacate, A method for the determination of dynamic resistance of photovoltaic
 243 modules under illumination, Technical Digest of the 14th International Photovoltaic Science and Engineering
 244 Conference—PVSEC 14, 26–30 January 2004, Bangkok, Thailand.
 245 [19].C.-H. Chang, Y. L. Lee, Appl. Phys. Lett. **91** (2007) 053503
 246 [20].J.Y. Kim, S.B. Choi, J.H. Noh, S.H. Yoon, S.W. Lee, T.H. Noh, A.J. Frank, K.S. Hong, Langmuir **25** (2009)
 247 5348.
 248 [21]. P. Sudhagar, J. H. Jung, S. Park, Y. G. Lee, R. Sathyamoorthy, Y. S. Kang, H. Ah. The performance of coupled
 249 (CdS:CdSe) quantum dot-sensitized TiO₂nanofibrous solar cells. Electrochemistry Communications **11** (2009)
 250 2220–2224.
 251 [22]. N. Balisa, V. Dracopoulosb, K. Bourikasc, P. Lianos. Quantum dot sensitized solar cells based on an optimized
 252 combination of ZnS, CdS and CdSe with CoS and CuS counter electrodes. ElectrochimicaActa**91** (2013) 246–252.
 253 [23]. G. V. Chris and J. Neugebauer, Nature **423**, 626 (2003).